Influence of testing method on mechanical properties of ceramic matrix composites

R. N. SINGH
General Electric Corporate Research and Development, Schenectady, NY 12301, USA

Mechanical properties of a monolithic zircon and zircon-matrix composites reinforced with silicon carbide monofilaments and/or whiskers were measured in three-point flexure and uniaxial tension modes to study the influence of testing methods on mechanical behaviour. A number of composite characteristics, such as the first-matrix cracking stress and strain, the ultimate composite strength and strain, and the modulus were obtained from the load–deflection behaviour in flexure and tension tests. The results indicated that the modulus values and the qualitative dependence of mechanical properties on composite parameters were similar in flexure and tension tests. In contrast, all of the other mechanical properties of the monolithic and composites were different in tests performed in flexure and tension modes. Typically, the first-matrix cracking stress and strain were higher in flexure tests than in tension tests, and these stress and strain values were independent of the filament–matrix interfacial properties. Similarly, the ultimate strengths of the monolithic and composites were higher in flexure than in tension, and these strengths were independent of interfacial properties. Therefore, the mechanical properties of composites obtained in flexure should not be used for a quantitative comparison with the predictions of micromechanical models, which are derived under the assumption of a uniform tensile stress. However, the flexure data are perfectly valid in demonstrating the qualitative dependence of mechanical properties on composite parameters.

1. Introduction
A tough and uniaxially reinforced ceramic-matrix composite, when subjected to a tensile loading in the direction of fibre reinforcement, is expected to display stress–strain or load–deflection behaviour as shown schematically in Fig. 1. An elastic behaviour is displayed in the initial stages followed by an extended regime showing an inelastic behaviour. There is a sudden load drop at the transition point from elastic to inelastic regime that is characterized by the first evidence of matrix cracking. Beyond this point, in the inelastic region, the slope of the load–deflection curve progressively decreases as the sample elongates because of filament failure and matrix microcracking. In spite of filament failures, the composite sample displays increasing load-bearing capacity reaching an ultimate in load-carrying capacity followed by a gradual load drop as an increasing number of filaments begin to break and pull out from the surrounding matrix phase. The first-matrix cracking stress, σ_{cr}, and strain, ε_{cr}, composite modulus, E, ultimate load-bearing stress, σ_u, and strain, ε_u, and work-of-fracture, WOF, i.e. the area under the load–deflection curve, are important material parameters that can be used to design with composite materials.

Application of ceramic-matrix composites in load-bearing structures requires a knowledge and determination of mechanical properties under testing conditions that simulate the actual loading environment. Typically, the mechanical behaviour of ceramic materials is modelled in tension but tested in either tension, compression, or flexure mode. The results of a tension test are most easily interpreted and modelled, but these tests are most difficult to perform. In contrast, flexure tests are easy to perform but the interpretation of data and its usefulness in modelling is considered more difficult because of a nonuniform stress/strain distribution within the specimen cross-section. A nonuniform stress distribution in flexure tests, as opposed to a uniform stress distribution in tension tests, makes it difficult to relate the results from one test to the other test. In spite of these difficulties, many studies have been performed on monolithic ceramics to assess the applicability of using flexure data in arriving at tensile properties. Such studies for fibre-reinforced ceramic composites are limited [1, 2]. Therefore, uniaxially fibre-reinforced ceramic-matrix composites were tested in a tension and in a flexure mode to determine the influence of testing methods on measured mechanical properties. A number of composite characteristics, such as the first-matrix cracking stress and strain, the ultimate composite strength and strain, and the modulus, were obtained from the load–deflection behaviour in tension and flexure modes. The mechanical properties of composites in tension and flexure were assessed and compared with similar measurements performed on the monolithic matrix phase. The validity of using

0022–2461/91 $03.00 + .12

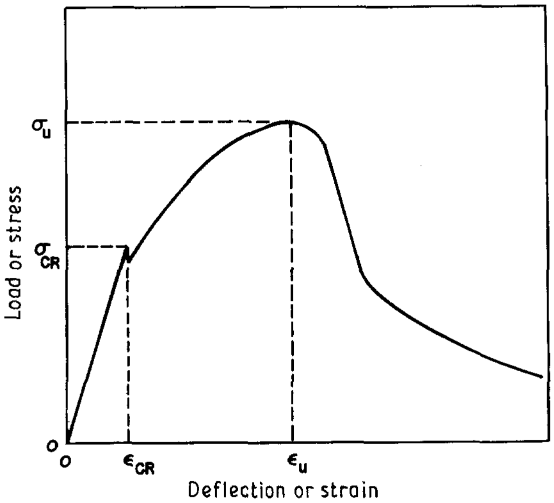

Figure 1 A schematic drawing showing load–deflection behaviour for a ceramic-matrix composite tested in uniaxial tension.

critical composite properties data, obtained from flexure tests, for comparison with the predictions of composite models is discussed.

2. Experimental procedure

Silicon carbide monofilaments (AVCO-SCS-6) and/or whiskers were used as reinforcements in the zircon ($ZrSiO_4$) matrix. These filaments have a diameter of 140 μm, an elastic modulus of 400 GPa, a strength of 3.4 GPa, and a failure strain between 0.8% and 1.0%. A silicon carbide whisker, Tateho SCW-1, was used as a discontinuous reinforcement of the zircon matrix. The crystal structure of this whisker was a cubic β-silicon carbide. Typical whisker diameter between 0.3 and 0.8 μm, length between 20 and 50 μm, and bulk density between 0.1 and 0.2 $g\,cm^{-3}$ were the physical characteristics of the as-supplied material. The silicon carbide whiskers were used in the as-supplied condition without any other classification treatments. The zircon matrix was prepared from a zircon powder (Zircon Flour, coarse-grained no. 51698).

The monolithic zircon and zircon composites reinforced with SiC filaments were fabricated by the steps described previously [3], and zircon composites reinforced with SiC filaments and/or whiskers were fabricated by a technique described in [4]. These steps produced fully dense composites with little porosity (< 1%). A typical fibre loading of 25% by volume was used in all the zircon–silicon carbide composites of this investigation. The composites with SiC whiskers and filaments had 25% by volume filament loading and 20% by volume whiskers in the matrix phase. An optical micrograph showing the cross-section normal to the filaments of a fully consolidated composite is shown in Fig. 2. It shows uniform distribution of filaments in a fully dense zircon matrix, and filaments are completely surrounded by the zircon matrix. Cross-sections of a number of composites were examined in this way, and none of the samples showed filament-to-filament contact, which can be deleterious to the composite properties. An average grain size of

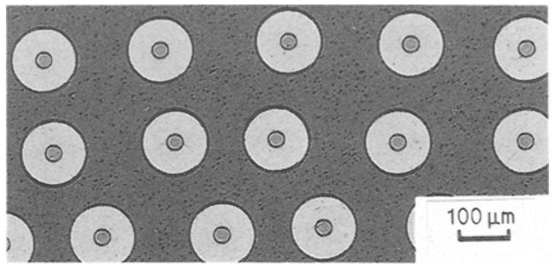

Figure 2 Optical micrograph showing a cross-section of a fully consolidated zircon–silicon carbide composite.

3 μm for the matrix phase comprised of either the zircon or the zircon with SiC whiskers was obtained.

Three types of fibre–matrix interfaces were created in the fully consolidated composites in order to study their influence on mechanical properties. In one case, as-supplied filaments containing the carbon-rich surface were used, and in another case, a boron nitride coating was deposited on the as-supplied filaments. The BN coating, about 1 μm thick, was deposited by a low-pressure chemical vapour deposition technique described elsewhere [5]. The interface between an as-supplied filament and the surrounding zircon matrix is designated interface A and that between a BN-coated filament and the surrounding zircon matrix is designated interface B. In addition, as-supplied SiC filaments were also incorporated into a zircon matrix containing SiC whiskers. The interface between an as-supplied SiC filament and the surrounding zircon matrix containing SiC whiskers is designated interface C.

Mechanical testing of the uniaxially reinforced composite was performed in three-point flexure and tension modes. All samples were individually hot-pressed and ground to a finish of 60 μm. Typical dimensions of the bar-shaped specimens for three-point flexure tests were 3.18 cm long, 0.79 cm wide, and 0.15 cm thick. The span of the lower support pins was 2.54 cm, which produced a span-to-thickness ratio of 16.9 in three-point flexure test mode. The flexure tests were performed in a universal testing machine at a crosshead speed of 0.0127 $cm\,min^{-1}$ (0.005 $in\,min^{-1}$). The deflection of the sample was measured from the crosshead motion, and the outer fibre strain was measured by a strain gauge mounted on the tensile surface at the midpoint between the lower support pins. The use of the strain gauge allowed for an accurate measurement of the first-matrix cracking strain. The load was measured by a load cell in the universal testing machine.

The samples for the tensile test were fabricated from the bar-shaped specimens, which were similar to those used in flexure tests. A gauge section of reduced cross-section was machined for tensile specimens using an ultrasonic machining technique. A picture of an initial tensile test specimen is shown in Fig. 3. It shows a flat rectangular area for gripping, which is connected to the reduced gauge section via a curved machined neck of either 0.254 or 0.635 cm radius of curvature. The gauge section was typically 0.5 cm long, 0.25 cm wide and 0.15 cm thick. Fibreglass-reinforced epoxy tabs were used for gripping; they were glued on both sides

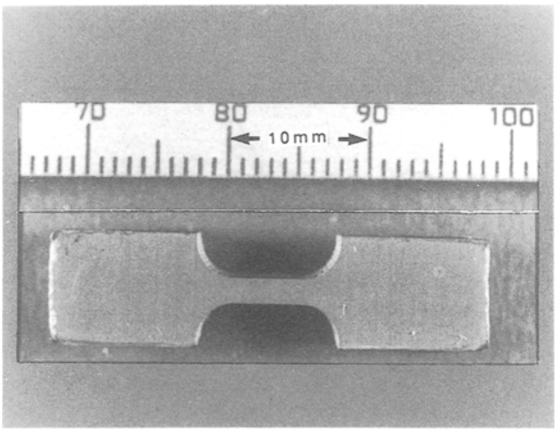

Figure 3 A tensile test sample with the single-stepped geometry separated by ultrasonic machining of the composite

of the flat tensile specimen using Permabond-910 adhesive. The samples were gripped using frictional grips, which worked very well and never allowed slippage or failures in the gripped area. The tensile sample was placed in the grips in such a way as to have good alignment of the tensile axis with the axis of the grips. The gripped sample was attached to the crossheads of a universal testing machine using self-aligning universal joints. The influence of specimen geometry, gripping, and aligning procedures on introduction of bending stresses was studied in this investigation. Optimum sample geometry and aligning procedures that minimized the introduction of bending stresses in tensile tests were obtained for reliable tension tests. The presence of bending stresses was measured and monitored by placing two strain gauges on opposite faces of the tensile gauge section. This also allowed for an accurate measurement of tensile strain during testing. The load was measured by a load cell attached to the testing machine. All of the tensile tests were performed in a universal testing machine at a crosshead speed of 0.0127 cm min^{-1} (0.005 in min^{-1}).

Load–deflection data were obtained in flexure and tension modes for a monolithic zircon and filament-reinforced composites until complete failure of the samples. The mode and location of failure were determined from visual observations during the test and scanning electron microscope (SEM) examinations of the failed samples subsequent to the test. The extent of filament pullout and the location of filament–matrix interfacial sliding were determined from examination of the fractured cross-section in an SEM.

3. Results and discussion

3.1. Mechanical properties in flexure

Monolithic zircon and zircon–SiC composites reinforced with SiC whiskers and/or filaments were tested in three-point flexure and tension modes, as described earlier. The load was measured by a load cell, and the strain was measured using strain gauges or calculated from the crosshead deflection. The load–deflection results in flexure for the monolithic zircon and zircon composites reinforced with as-supplied and BN-coated SiC filaments are shown in Fig. 4. Monolithic zircon displayed brittle behaviour and had a strength value of 267 MPa. The strain to failure of 0.13% for this sample was measured using a strain gauge. In contrast, the composite samples showed a toughened composite-like behaviour from which the critical stress for first-matrix cracking was determined. One sample reinforced with as-supplied SiC filaments gave a value of 260 MPa for the critical stress for first-matrix cracking and a corresponding strain value of 0.11%. Another sample reinforced with BN-coated SiC filaments produced a matrix cracking stress value of 385 MPa and a corresponding strain value of 0.13%. Both the composite samples displayed a significant amount of load-carrying capability beyond the first-matrix cracking stress and resulted in ultimate strength values of 689 and 712 MPa, respectively, for composites reinforced with as-supplied and BN-coated SiC filaments. The strain values corresponding to ultimate strength could not be measured by the strain gauge because of their failure as a result of the matrix cracking, but the ultimate failure strains calculated from deflection data gave values of 1.2% and 1.04%, respectively, for composites reinforced with as-supplied and BN-coated filaments. The composite reinforced with BN-coated filaments showed a gradual load drop beyond the point of maximum load. In contrast, the composite reinforced with as-supplied filaments showed a sudden load drop beyond the point of maximum load.

The elastic modulus values of 201 GPa for a monolithic zircon, 237 GPa for the composite reinforced with as-supplied filaments, and 259 GPa for the composite reinforced with BN-coated filaments were measured from the slope of the linear portion of the load–deflection data shown in Fig. 4. These mechanical property data for a monolithic zircon and zircon–SiC composites are very close to average mechanical properties calculated from the load and crosshead displacement data obtained in three-point flexure tests, as summarized in Table I. For example, the critical strain for matrix cracking as measured by a strain gauge ranged between 0.11% and 0.13% for monolithic and composite samples, which are similar to values of between 0.11% and 0.15% as calculated from the crosshead displacement data. Similarly, the elastic moduli calculated from the ratio of σ_{cr} and ε_{cr}, in which the strain value was determined by a strain gauge, are close to the modulus values calculated from the slopes of the elastic portion of the load–deflection data after subtracting out the deflection because of the machine compliance.

Incorporation of SiC whiskers into the zircon matrix has been shown to enhance critical stress for first-matrix cracking of filament-reinforced composites [4]. These composites were also tested in this study to determine mechanical property data. The load–deflection results obtained for a zircon sample reinforced with SiC whiskers or with SiC whiskers and filaments are shown in Fig. 5. The zircon composite reinforced with SiC whiskers failed in a brittle manner that is typical of the monolithic ceramics and had a strength of 353 MPa, which is much higher than the strength of

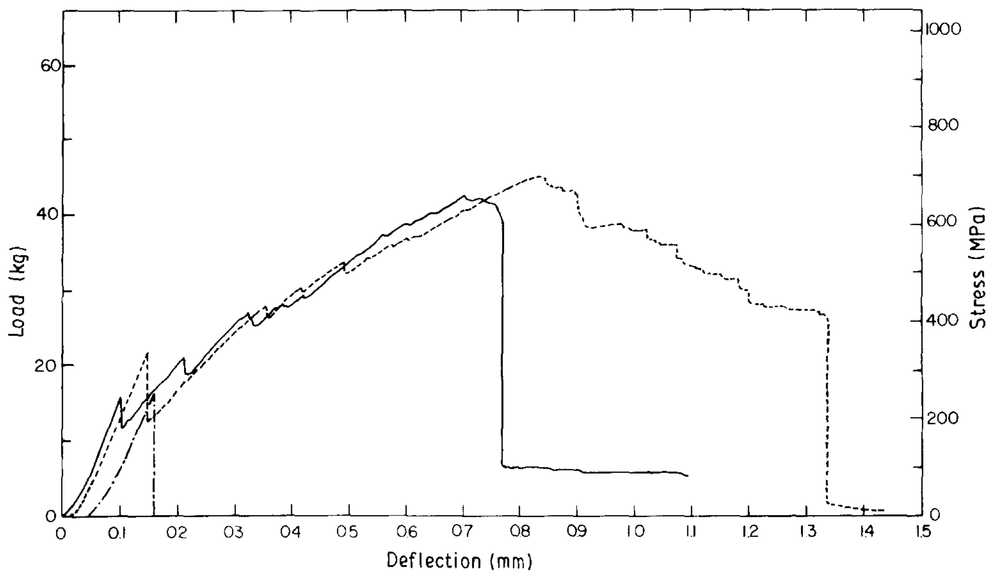

Figure 4 Load–deflection behaviour obtained flexure tests for (—· –) a monolithic zircon and zircon composites reinforced with either as-supplied or BN-coated silicon carbide filaments. (——) Zircon–AVCO SiC composite (interface A), (---) zircon-AVCO SiC composite (interface C).

TABLE I A summary of mechanical properties in flexure for monolithic zircon and zircon–SiC composites reinforced with SiC whiskers and/or filaments

Composite constituents			Filament–matrix interface	Mechanical properties in flexure				
Matrix	Filament	Whisker		σ_{cr} (MPa)	ε_{cr} (%)	E (GPa)	σ_u (MPa)	ε_u (%)
Zircon	–	–	None	281 ± 88	0.15 ± 0.02	195 ± 23	281 ± 88	0.15 ± 0.02
Zircon	–	–	None	267	0.13[a]	201	267	0.13[a]
Zircon	SiC	–	A	287 ± 28	0.11 ± 0.01	244 ± 6	700 ± 56	1.08 ± 0.13
Zircon	SiC	–	A	260	0.11[a]	237	689	1.2
Zircon	SiC	–	B	357 ± 43	0.14 ± 0.03	235 ± 26	681 ± 36	1.06 ± 0.30
Zircon	SiC	–	B	385	0.13[a]	259	712	1.04
Zircon	–	SiC	None	342 ± 15	0.23 ± 0.02	154 ± 21	342 ± 15	0.23 ± 0.02
Zircon	–	SiC	None	347	0.21[a]	142	347	0.21[a]
Zircon	SiC	SiC	C	441 ± 29	0.24 ± 0.02	183 ± 14	647 ± 17	1.27 ± 0.35
Zircon	SiC	SiC	C	405	0.21[a]	197	629	0.90

[a] Critical strain for matrix cracking was measured by strain gauge.

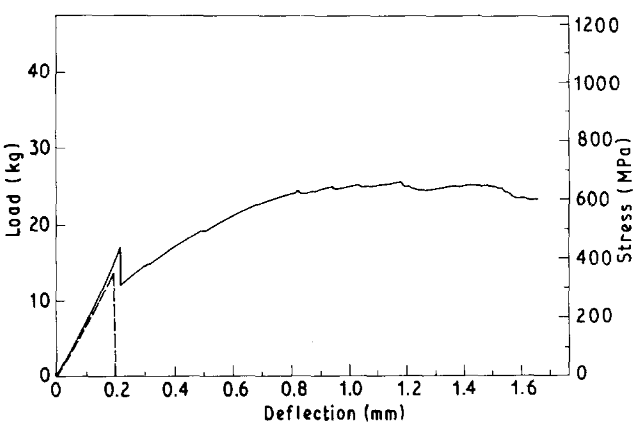

Figure 5 Load–deflection behaviour obtained in flexure for zircon composites reinforced with either (– – –) SiC whiskers or (——) SiC whiskers and as-supplied SiC filaments (interface C)

the monolithic zircon. In contrast, a zircon composite reinforced with SiC whiskers and filaments showed toughened composite-like behaviour with a matrix cracking stress of 434 MPa and an ultimate strength of 656 MPa. An average failure strain of 0.23% was measured for samples reinforced with SiC whiskers, which is close to the failure strain of 0.21% as measured by a strain gauge. Similarly, a composite sample reinforced with SiC whiskers and filaments produced a critical matrix cracking strain of 0.21% when measured by a strain gauge, which is also close to the average matrix cracking strain of 0.24% measured from the crosshead deflection data. These results indicate that the matrix cracking strain measured by crosshead deflection data and by strain gauges are very close to each other in tests performed in flexure.

An average elastic modulus of 154 MPa for whisker-reinforced zircon and an average modulus of 183 GPa for whisker- and filament-reinforced zircon composites were obtained from the slope of the elastic portion of the load–deflection curves. These moduli are very close to values calculated from the ratio $\sigma_{cr}/\varepsilon_{cr}$ in which the critical strain for matrix cracking was determined by a strain gauge. These results obtained in flexure appear to be fairly self-consistent and follow the rule-of-mixture predictions for elastic modulus [3, 4]. In addition, it appears that the matrix cracking stress in this class of composites is determined by the failure strain of the matrix, which is not enhanced above the monolithic matrix failure strain because of reinforcement by the SiC monofilaments [6]. An increase in matrix cracking stress, from a value of 342 MPa for samples reinforced with SiC whiskers to a value of 441 MPa for composites reinforced with SiC whiskers and filaments, can be attributed to enhanced modulus value because the critical strain for first-matrix cracking was nominally the same.

The cross-section of a composite sample tested in three-point flexure was examined in an SEM to determine the nature of the fracture process. A scanning electron micrograph of the as-fractured surface of a zircon composite reinforced with SiC whiskers and filaments is shown in Fig. 6. Filament pullout, debonded filament–matrix interface, and a rough fractured surface are evident. Also evident is a nonplanar propagation of the crack front because of crack deflection by the reinforcing filaments. These observations suggest that toughening in zircon–SiC composites is via a combination of fibre pullout, crack deflection, and possibly microcracking mechanisms. The interfacial sliding was observed to occur at two different locations on the same filament, as shown in Fig. 6b. Part of the sliding occurs between the outer filament surface and the zircon matrix, and then the crack propagates through the carbon coatings, with further sliding occurring between the inner carbon coating and the SiC surface that comprise the bulk of the SiC filament. A similar behaviour for the location of interfacial sliding was observed for zircon composites reinforced with uncoated or BN-coated SiC filaments, and those composites reinforced with SiC whiskers and filaments.

3.2. Mechanical properties in tension

The initial results of the tension tests were quite variable in comparison with the fairly consistent data obtained in flexure tests. A number of factors contributed to this variability, such as sample geometry, compliance of the gripping system, alignment of the test fixture, and effect of the off-axis loading. These factors were systematically studied, as described below.

The first set of tests was performed on flat bar-shaped samples, similar to those used for flexure tests. Fibreglass-reinforced epoxy tabs were attached to each specimen for gripping and the specimens were then pulled in uniaxial tension in a direction parallel to the reinforcing filaments. Application of loads beyond about 500 kg led to deformation of the tabs and did not lead to fracture of the sample. This is not unreasonable because a load of about 800 kg is required to fracture a composite with an ultimate strength approaching 700 MPa. Therefore, samples with another geometry containing a reduced gauge section were fabricated to enable composite fracture within a maximum load of about 500 kg. This specimen geometry consisted of a single-stepped region having a uniform gauge section about 5 mm long, 2.5 mm wide, and 1.5 mm thick, as shown in Fig. 3. Epoxy tabs were placed on both sides of the flat ends for gripping and a metal strain gauge was attached on one side of the gauge section to measure strain. This sample was then placed in a jig and the epoxy-ends were gripped with friction grips. Then, this sample was connected to the crossheads of a universal testing machine via a variety of fixtures ranging from chain links to a progressively more rigid fixture to avoid the presence of bending stresses. Invariably, monolithic and composite samples failed at the start of the gauge section, and the failure strain measured by a strain gauge ranged between 0.06% and 0.09%. The value of elastic modulus calculated from matrix cracking stress and strain was much higher than the expected modulus for these samples. Because of this behaviour, attempts were made to measure systematically bending stresses and to eliminate these from tensile test results.

The presence of a bending stress in tension tests was measured with the application of two strain gauges (one on each surface) on a mild-steel sample of approximately the same thickness as the tensile test specimen. This sample was then gripped at the tab area in a manner similar to that used for composite samples and pulled in a universal testing machine within the elastic region of the steel sample. The load and strain values were continuously monitored using a load cell and strain gauges. The influence of the fixture attachment method on measured strain values

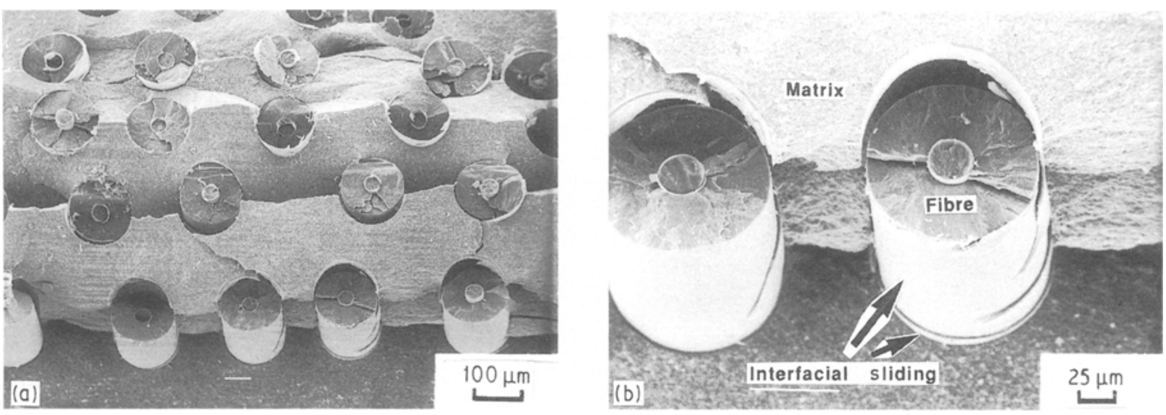

Figure 6 Failed cross-section of a Zircon–SiC whisker–SiC filament composite tested in three-point flexure showing filament pullout, interfacial sliding, and a nonplanar matrix fracture.

is shown in Fig. 7. The first set of experiments used chain links for attaching a specimen fixture to the crosshead, which produced a significant amount of bending stresses as is evident by the compressive and tensile nature of the measured strains from opposite faces of the steel specimen. The second set of experiments was performed using a more rigid fixture in which some of the linkages were loose. This produced opposite strains in the early stages of the loading, but at higher loads both sides of the specimen produced tensile strains. The strain values from different faces of the same sample were still unequal. The third set of experiments used the same fixture as in the second trial but all of the linkages were made rigid, which produced tensile strains from both sides of the steel sample. In addition, the strain values from both surfaces were very close to each other, as shown in Fig. 7. An elastic modulus of 200 GPa was calculated from the stress and strain values measured on the steel sample. This value is in good agreement with the modulus value for a mild-steel specimen. These procedures were always performed before each of the composite testings in order to align the test-fixture and to avoid bending stresses. The composite samples were then placed in the test fixture and preloaded to check the alignment via measuring strain using two strain gauges mounted on the opposite faces. The real tests were only performed when both of the strain gauges produced tensile values very close to each

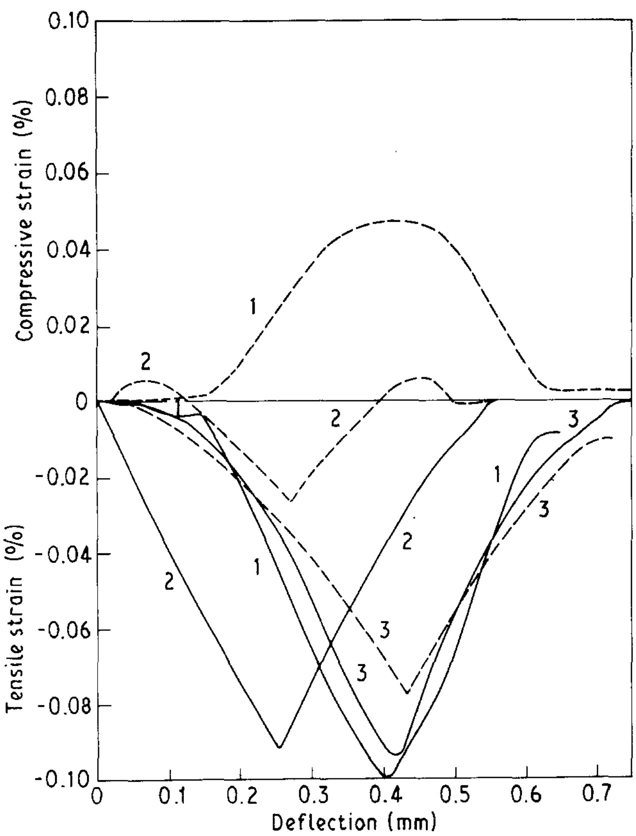

Figure 7 Strain–deflection data, obtained from opposite faces of a mild-steel tensile specimen in tension tests, showing the influence of test-fixturing on production of a nonuniform bending strain. Curves labelled 1 utilized chain-links and those labelled 2 and 3 utilized a progressively more rigid fixturing. Strain gauge position (——) back surface, (- - -) front surface.

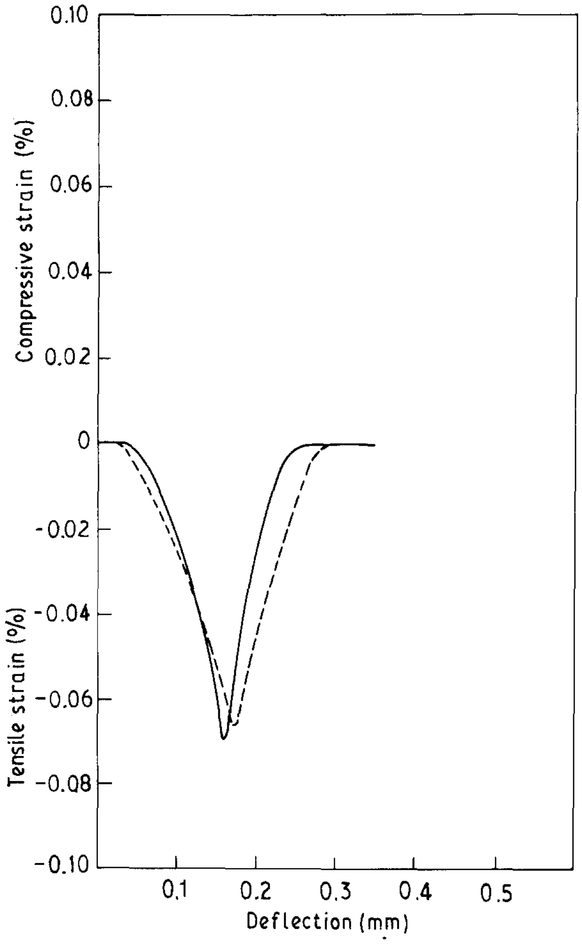

Figure 8 Strain–deflection data, obtained from opposite faces of a zircon–SiC whisker–SiC filament composite specimen showing a uniformly stressed sample in a tensile test. Proper aligning procedures were utilized in this test to eliminate bending stresses. Strain gauge position as in Fig. 7.

other, as is shown in Fig. 8, for one of these tensile tests performed on a fibre-reinforced composite.

Monolithic and composite ceramics, having specimen geometry as given in Fig. 2 and using all the alignment procedures described above, were fractured in tension. The fracture was still found to be at the start of the necked gauge section rather than in the middle of the gauge section. This can be attributed to the stress concentration near the start of the gauge section because of the re-entrant corner. The corresponding matrix cracking strain values measured on these samples were much lower than the values obtained in flexure tests and were quite variable, as shown in Table II. This behaviour may be because of the location of the strain gauge, which was at times away from the location of matrix cracking. In order to enhance matrix cracking in the gauge section, another sample geometry having a double-stepped region leading into the gauge section, as shown in Fig. 9, was used. This sample geometry resulted in matrix cracking within the gauge section and produced much higher and more consistent values of the critical strain for first-matrix cracking in comparison to that using a single-stepped geometry, as also given in Table II. Therefore, it is important to reduce bending stresses and produce failure near the strain gauges in order to make valid stress and strain measurements in a tensile test.

TABLE II Influence of specimen geometry on tensile mechanical properties of zircon composites reinforced with SiC whiskers and/or filaments

Composite constituents			Filament–matrix interface	Specimen geometry	Mechanical properties in tension		
Matrix	Filament	Whisker			σ_{cr} (MPa)	ε_{cr}^{a} (%)	σ_u (MPa)
Zircon	–	SiC	None	Single-stepped	185	0.09	185
Zircon	–	SiC	None	Double-stepped	258	0.17	258
Zircon	SiC	SiC	C	Single-stepped	320	0.06	405
Zircon	SiC	SiC	C	Double-stepped	387	0.21	512

[a] Critical strain for matrix cracking was measured by strain gauge.

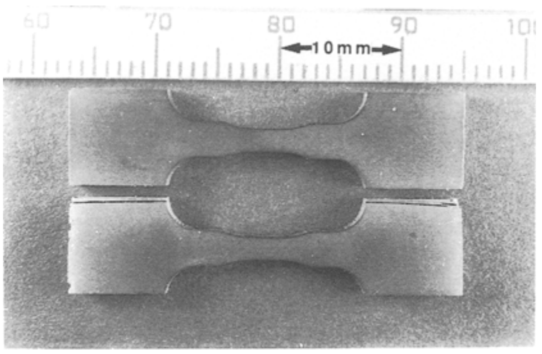

Figure 9 Tensile test specimens with the double-stepped geometry prepared by ultrasonic machining.

The rest of the tensile tests in this study were performed on ceramic specimens with double-stepped geometry, and all of the procedures described above were followed for avoiding the bending stresses. The tensile tests were performed on samples of a monolithic zircon and zircon composites reinforced with SiC whiskers and/or filaments. The load–deflection data for a monolithic zircon and zircon–SiC composites reinforced with as-supplied and BN-coated SiC filaments are shown in Fig. 10. The monolithic sample fractured in a brittle manner and had a strength of 216 MPa. In contrast, both of the composite samples displayed toughened composite-like behaviour with matrix cracking stress very similar to the monolithic zircon in spite of the fact that the BN-coated filaments produced lower interfacial shear stress [7]. The ultimate strength of these composites ranged between 430 and 546 MPa. Both of the composite samples containing either as-supplied or BN-coated filaments displayed a sudden load drop after reaching the ultimate strength in tension tests, which is different from the results obtained in flexure tests. In particular, composites reinforced with BN-coated filaments and tested in flexure showed a much more gradual drop in load after reaching the point of maximum load-carrying capacity. The nature of the tensile load–deflection curves for composites reinforced with SiC whiskers and filaments was essentially similar to those for composites reinforced with only SiC filaments (Fig. 10), except that the stress and strain values were different.

A summary of the mechanical properties of the monolithic and composite samples tested in tension is given in Table III. The results are divided into two groups depending on the type of composite material. The first group is for monolithic zircon and zircon–SiC composites reinforced with as-supplied and BN-coated filaments, and the second group is for zircon composite reinforced with SiC whiskers and zircon composite reinforced with SiC whiskers and filaments. The results for the first group show that the modulus values calculated from the ratio of matrix cracking stress and matrix cracking strain (measured by a strain gauge) are very close to modulus values measured in three-point flexure tests (see Table I). For example, the monolithic zircon sample failed at a stress of 216 MPa and a strain of 0.11% and resulted in a modulus of 196 GPa, which is very close to an average modulus value of 195 GPa measured in flexure. Similarly, a modulus value of 247 GPa for the zircon composite reinforced with as-supplied filaments, and a modulus value of 259 GPa for the zircon composite reinforced with BN-coated filaments were measured from matrix cracking stress and strain values. Again, these moduli are similar to those measured in flexure. Therefore, the matrix cracking strain in tension tests can be obtained from the ratio of the matrix cracking stress measured in tension and the modulus value measured in flexure. The average value of matrix cracking strain measured by this procedure is 0.09% for composites reinforced with as-supplied SiC filaments, and an average value of 0.10% is obtained for composites reinforced with BN-coated filaments. The ultimate composite strength in tension was 519 MPa for specimens reinforced with as-supplied filaments and an average value of 470 MPa was obtained for composites reinforced with BN-coated filaments.

Composites reinforced with SiC whiskers and/or filaments behaved in a manner similar to those reinforced with SiC filaments alone with some important differences, as summarized in Table III. The moduli calculated from the ratio of matrix cracking stress and strain were similar to those measured in flexure, but the magnitude of matrix cracking stress and strain was higher than the composites reinforced with only SiC filaments. For example, zircon matrix reinforced with SiC whiskers failed at an average stress of 258 MPa and at an average strain of 0.17%,

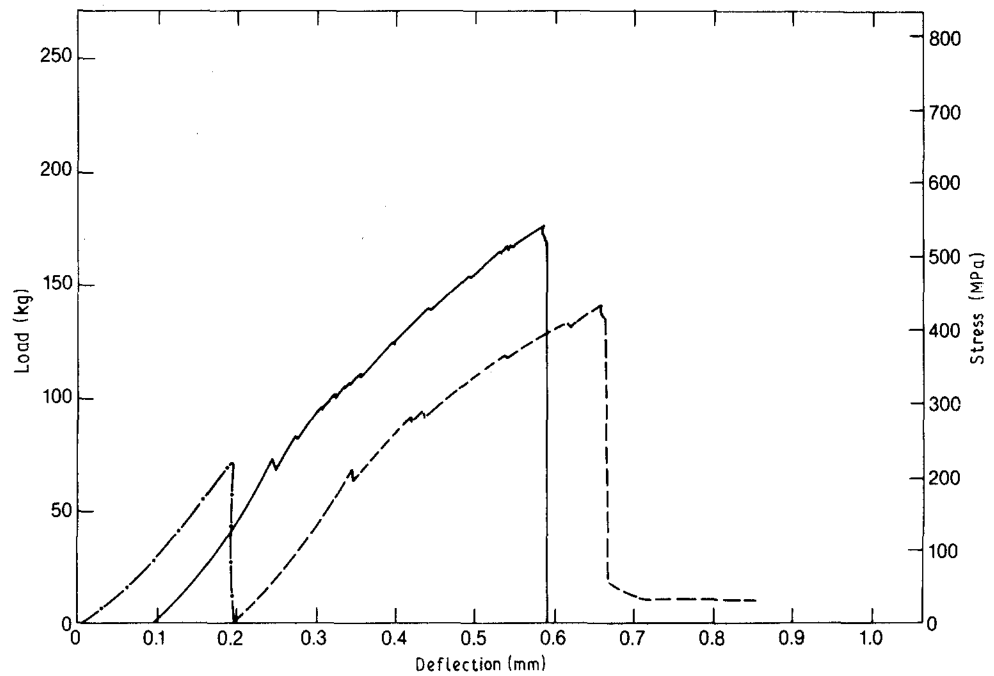

Figure 10 Load–deflection behaviour obtained in tension tests for (—·—) a monolithic zircon and zircon composites reinforced with either as-supplied or BN-coated silicon carbide filaments. (——) Zircon–SiC filament composite (interface A), (---) zircon–SiC filament composite (interface B).

TABLE III A summary of mechanical properties in tension for monolithic zircon and zircon–SiC composites reinforced with SiC whiskers and/or filaments

Composite constituents			Filament–matrix interface	Mechanical properties in tension			
Matrix	Filament	Whisker		σ_{cr} (MPa)	ε_{cr} (%)	E^a (GPa)	σ_u (MPa)
Zircon	–	–	None	216 ± 18	$0.11^b \pm 0.01$	196	216 ± 18
Zircon	SiC	–	A	217 ± 15	0.09 ± 0.01	244	519 ± 38
Zircon	SiC	–	A	227	0.09^b	252	546
Zircon	SiC	–	B	220 ± 27	0.10 ± 0.01	235	470 ± 87
Zircon	SiC	–	B	203	0.09^b	226	568
Zircon	–	SiC	None	258 ± 20	0.17 ± 0.06	154	258 ± 20
Zircon	–	SiC	None	330	0.21^b	157	330
Zircon	SiC	SiC	C	333 ± 45	0.18 ± 0.03	183	463 ± 67
Zircon	SiC	SiC	C	387	0.21^b	184	512

[a] Elastic modulus in tension was taken to be the same as in flexure or calculated from $\sigma_{cr}/\varepsilon_{cr}$.
[b] Critical strain for matrix cracking was measured by strain gauge.

both of which are higher than the failure stress of 216 MPa and failure strain of 0.11% measured for monolithic zircon. Similarly, zircon composites reinforced with SiC whiskers and filaments displayed an average matrix cracking stress of 333 MPa and corresponding matrix cracking strain of 0.18%. The increase in matrix cracking stress in filament- and whisker-reinforced composites in comparison to the zircon composite containing whiskers only can be attributed to higher modulus value of 183 GPa for filament-reinforced specimens with nominally the same matrix cracking strain of 0.18%. The increase in matrix cracking stress, in whisker-reinforced composites in comparison to a monolithic zircon or zircon composites reinforced with SiC filaments, can be attributed to higher strain to failure of the matrix phase in whisker- and filament-containing composites. The ultimate strength of SiC whisker- and filament-reinforced zircon in tension is 463 MPa.

The fractured cross-sections of composite samples tested in tension were examined by SEM to determine the extent of fibre pullout and fracture morphology. Scanning electron micrographs from such a specimen are shown in Fig. 11. Fig. 11a shows the nature and the extent of fibre pullout. The fibre pullout length is approximately equal to a filament diameter. The fractured matrix surface appears to be fairly planar for samples tested in tension (Fig. 11a) in comparison to the matrix fracture surface for samples tested in flexure (Fig. 6a). This appears to be because of different modes of fracture for samples tested in tension and in flexure. In tension, the composite failure was observed to be a result of one major crack whereas in the case of flexure tests the composite failure was observed to be caused by multiple matrix cracking. Multiple matrix cracking in flexure tests is expected to result in a more uniform and lower level of localized stresses on the crack-bridging filaments, and as a consequence the com-

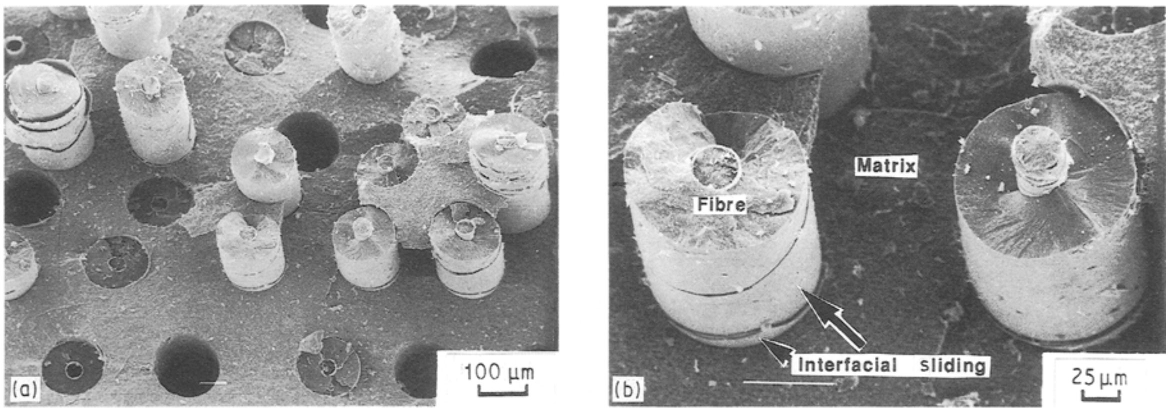

Figure 11 Failed cross-section of a zircon–SiC whisker–SiC filament composite tested in tension showing filament pullout, interfacial sliding, and a planar matrix fracture.

posite samples are expected to show higher ultimate strengths than those for samples tested in tension. The fibre–matrix interfacial sliding was observed at two locations. A part of the interfacial sliding was between the zircon matrix and the outer surface of the SiC filament, and then the crack front fractured the two layers of carbon coating and propagated between the inner carbon coating and the SiC layer that comprises the bulk of the SiC filament, as shown in Fig. 11b.

3.3. Comparison of mechanical properties in flexure and tension tests

A number of composite characteristics, such as the load–deflection behaviour, critical stress and strain for first-matrix cracking, ultimate composite strength, and composite modulus were compared for tests performed in either a flexure or a tension mode. Qualitatively, the nature of load–deflection curves obtained in flexure and tension tests was similar up to the point of maximum load-carrying capacity. Typically, both types of test displayed an initial elastic behaviour up to the point of first-matrix cracking, a sudden drop in load at the point of matrix cracking, and then an inelastic regime up to the point of maximum load-carrying capacity. In contrast, different behaviour was seen beyond the point of maximum load-carrying capacity for specimens tested in either flexure or tension mode. Flexure test results displayed either a sudden or a gradual load drop depending on the type of the fibre–matrix interface. Generally, zircon composites reinforced with uncoated SiC filaments (higher interfacial shear stress [7]) showed a complete loss of load-carrying capacity, whereas composites reinforced with BN-coated filaments (lower interfacial shear stress [7]) showed a gradual drop in load beyond the maximum point. In contrast, these same composites when tested in tension displayed complete loss in load-carrying capacity beyond the maximum point whether reinforced with uncoated or BN-coated filaments. A similar load–deflection behaviour was also shown by composites reinforced with SiC whiskers and uncoated SiC filaments.

A comparison is also made in Table IV of all the other mechanical properties that were obtained in flexure and tension tests of a monolithic zircon and composites reinforced with SiC whiskers and/or filaments. The monolithic zircon and composites showed higher values of first-matrix cracking strength in flexure than in tension tests. Zircon composites reinforced with either uncoated or BN-coated SiC filaments produced similar values of tensile matrix cracking strength. These matrix cracking strengths for composites were similar to the strength of a monolithic zircon. Composites reinforced with SiC whiskers and uncoated SiC filaments produced higher values of first-matrix cracking strength than the composites reinforced with only SiC filaments. However, again the matrix cracking strength in flexure was higher than that in tension. Corresponding values of the matrix cracking strain were also higher in flexure tests in comparison to tests performed in tension, and the matrix cracking strains of filament-reinforced composites were similar to failure strains of the monolithic

TABLE IV A comparison of average mechanical properties of a monolithic and composites measured in flexure (F) and tension (T) tests

Composite constituents			Filament–matrix interface properties		Mechanical properties							
Matrix	Filament	Whisker			σ_{cr}(MPa)		ε_{cr}(%)		E(GPa)		σ_u(MPa)	
			Type	τ^a(MPa)	F	T	F	T	F	T	F	T
Zircon	–	–	None	–	281	216	0.15	0.11	195	196	281	216
Zircon	SiC	–	A	39	287	217	0.11	0.09	244	244	700	519
Zircon	SiC	–	B	18	357	220	0.14	0.10	235	235	681	470
Zircon	–	SiC	None	–	342	258	0.23	0.17	154	154	342	258
Zircon	SiC	SiC	C	4.4	441	333	0.24	0.18	183	183	647	463

[a] τ is the first-push interfacial shear stress.

matrix phase. This behaviour indicated that filament reinforcement of the zircon matrix led to toughened composite-like behaviour, but it did not enhance the strain for matrix cracking in this class of composite sample [6]. Composites reinforced with SiC whiskers produced higher values of the matrix cracking strain in comparison to a monolithic zircon. This higher matrix cracking strain was responsible for the higher matrix cracking strength in whisker-reinforced composites in comparison to composites reinforced with only SiC filaments.

Composite moduli measured in flexure were similar to those measured in tension tests, and followed the rule-of-mixtures [3, 4]. The modulus values measured in tension were obtained from the ratio of matrix cracking stress and the corresponding matrix cracking strain. Generally, reinforcement of the zircon matrix or the zircon matrix containing SiC whiskers by the SiC filaments produced modulus values higher than those of the matrix phase. These higher modulus values for the filament-reinforced composite along with the corresponding strain values for matrix cracking contributed to higher matrix cracking strengths of filament-reinforced composites in comparison to strength of the monolithic matrix phase, as discussed before.

The ultimate strength of monolithic and composite samples was higher in flexure tests than in tension tests. This result was observed for a monolithic zircon and zircon composites reinforced with SiC whiskers and/or filaments. Typically, the ultimate strength in tension was 70%–75% of the strength values in flexure for both the monolithic and composite samples. The ultimate strength of a monolithic zircon was increased by the incorporation of SiC whiskers, but the ultimate strength of filament-reinforced composites was similar irrespective of whether the zircon matrix phase was reinforced with SiC whiskers or not. Similarly, the ultimate strength of filament-reinforced composites was independent of interfacial properties. For example, zircon composites reinforced with either uncoated or BN-coated filaments and composites reinforced with SiC whiskers and filaments produced filament–matrix interfacial shear stress between 4.4 and 39 MPa, and yet the ultimate strengths of these composites were between 463 and 519 MPa. These strength values are similar considering the standard deviation (Table III). These results seem to indicate that the ultimate strength of filament-reinforced composites is controlled by the ultimate strength characteristics of the reinforcing filaments rather than the interfacial properties or the strength of the matrix phase.

A lower value of strength in tension than in flexure has been observed for monolithic ceramic materials by other investigators. This is generally considered to be a result of different stress distributions in samples tested in tension and in flexure modes. In tension, the whole gauge section is subjected to a uniform tensile loading, whereas in three-point flexure only a thin sheet of material is subjected to tension. Because the strength of ceramic materials is dependent on sample size, it is not unreasonable to expect a lower strength value when samples are tested in tension than when tested in flexure. Similar arguments can be used to explain the lower strength of composites in tension tests in comparison to strength values obtained in flexure tests, because even the SiC reinforcing filaments have shown lower strength in tension than in flexure. Typically, the filament strength in tension was 70% of the strength in flexure [8].

One of the objectives of this study was to assess the validity of using mechanical property data that were obtained in flexure for comparison with predictions of micromechanical models, which are derived under the assumption of a uniaxial tensile loading. The results summarized in Table IV clearly suggest that except for the elastic modulus, most of the other mechanical properties of monolithic and composite samples were sufficiently different in flexure and tension tests. However, similar dependences of mechanical properties on composite parameters are qualitatively shown by data obtained in flexure and tension tests. Thus, these observations suggest that the results from flexure tests can be used to qualitatively assess the influence of composite parameters on mechanical properties, but the flexure data cannot be used for the quantitative comparison with the predictions of micromechanical models.

The testing of ceramic samples in tension is more difficult than that in flexure because of a number of problems. The most important of these is the possible presence of bending stresses because of the nonaxial loading of samples. This can result in a nonuniform stress and hence a nonuniform strain distribution on different faces of a flat tensile test specimen used in this study. The application of two strain gauges, one on each side of the test specimen, was used to monitor the presence of bending stresses during a tensile test. The testing fixtures were then adjusted to eliminate bending stresses from tensile tests. There is also the possibility of stress concentration at the transition from the gripped ends to the reduced gauge section of specimens because the transition from the large gripped ends to the small gauge section constitutes a reentrant corner which, according to the theory of elasticity, will always result in a stress concentration. A common practice for reducing the stress concentration is to approach the gauge section in two or more steps. This approach was also tried in tensile tests of this study which, along with the elimination of bending stresses, resulted in valid and consistent tensile data on composite and monolithic samples. In contrast, the consistent flexure data were easier to obtain than the tensile data.

4. Conclusions

Mechanical properties of monolithic zircon and zircon composites reinforced with SiC whiskers and/or filaments were measured in three-point flexure and tension modes. The following conclusions are made based on this study.

1. The flexure tests were easy to perform and produced fairly consistent mechanical properties. In contrast, tension tests were more difficult to perform and

produced inconsistent mechanical properties until the influence of bending stresses and stress concentrations was eliminated.

2. Application of strain gauges, mounted on the opposite faces of a flat tensile specimen, was used to monitor strains and hence the presence of bending stresses. The presence of bending stresses was then eliminated by specimen aligning procedures. In addition, a double-stepped specimen geometry reduced the stress concentration and enhanced sample failure in the reduced gauge section. These procedures resulted in more consistent tensile mechanical properties of the monolithic and composite samples.

3. The elastic moduli of a monolithic zircon and SiC filament-reinforced zircon composites were similar in flexure and tension tests, and followed rule-of-mixture predictions.

4. The first-matrix cracking stress and corresponding strain values measured in flexure were always higher than those measured in tension. Typically, the strength and strain in tension were about 70%–75% of the corresponding values in flexure. Similarly, the ultimate strengths of a monolithic zircon and zircon composites reinforced with SiC whiskers and/or filaments in tension were 69%–75% of the strengths in flexure.

5. The ultimate strengths of all composites tested in this study were similar in spite of the different interfacial and matrix properties. This behaviour indicated that the ultimate strength of these composites is controlled by the properties of the continuous reinforcement phase.

6. The first-matrix cracking strengths, obtained in tension and flexure for filament-reinforced composites, were independent of the filament–matrix interfacial shear stress. However, a direct dependence of the first-matrix cracking strength on the first-matrix cracking strain was observed.

7. The dependence of mechanical properties of composite on composite parameters was qualitatively similar for tests performed in tension and flexure modes. However, the mechanical property data obtained in flexure tests cannot be used in a quantitative comparison with the predictions of micromechanical models that are derived under the assumption of a uniform tensile loading.

Acknowledgements

The author thanks W. A. Morrison for help in sample preparation, C. Canestraro for help in mechanical testing, P. M. Breslin for manuscript preparation, and Drs K. L. Luthra, M. K. Brun and G. C. Corman for making useful comments.

References

1. T. MAH, M. G. MENDIRATTA, A. P. KATZ, R. RUH and K. S. MAZDIYASNI, *J. Amer. Ceram. Soc.* **68** (1985) C-27.
2. D. B. MARSHALL and A. G. EVANS, *ibid.* **68** (1985) 225.
3. R. N. SINGH and A. R. GADDIPATI, *J. Mater. Sci.* **25** (1990).
4. R. N. SINGH, *ibid.* **26** (1991).
5. *Idem.*, in "Proceedings of the Tenth International Conference on Chemical Vapor Deposition" (CVD-X), Honolulu, Hawaü Vol. 87-7 edited by G. W. Cullen (The Electrochemical Society, 1987) p. 543.
6. *Idem.*, *J. Amer. Ceram. Soc.* **73** (1990) 2930.
7. *Idem.*, *ibid.* **72** (1989) 764.
8. P. A. SIEMERS and R. L. MEHAN, *J. Mater. Sci.* **23** (1988) 1329.

Received 23 April
and accepted 6 November 1990